



# Linking tundra vegetation, snow, soil temperature, and permafrost

Inge Grünberg<sup>1</sup>, Evan J. Wilcox<sup>2</sup>, Simon Zwieback<sup>3</sup>, Philip Marsh<sup>2</sup>, and Julia Boike<sup>1,4</sup>

<sup>1</sup>Permafrost Research, Alfred-Wegener-Institut für Polar und Meeresforschung, Potsdam, Germany

<sup>2</sup>Cold Regions Research Centre, Wilfrid Laurier University, Waterloo, ON, Canada

<sup>3</sup>Geophysical Institute, University of Alaska Fairbanks, Fairbanks, AK, United States

<sup>4</sup>Humboldt-Universität zu Berlin, Berlin, Germany

**Correspondence:** I. Grünberg (inge.gruenberg@awi.de)

**Abstract.** Soil temperatures in permafrost regions are highly heterogeneous on small scales, in part due to variable snow and vegetation cover. Moreover, the temperature distribution that results from the interplay of complex biophysical processes remains poorly constrained. Sixty-eight temperature loggers were installed to record the distribution of topsoil temperatures at the Trail Valley Creek study site in the Northwestern Canadian Arctic. The measurements were distributed across six different  
5 vegetation types characteristic for this landscape. Two years of topsoil temperature data were analysed statistically to identify temporal and spatial characteristics and their relationship to vegetation, snow cover and active layer thickness. The mean annual topsoil temperature varied between  $-3.7^{\circ}\text{C}$  and  $0.1^{\circ}\text{C}$  within a 1.2 km distance, with an approximate average across the landscape of  $-2.3^{\circ}\text{C}$  in 2017 and  $-1.7^{\circ}\text{C}$  in 2018. The observed variation can, to a large degree, be explained by variation  
10 in snow cover. Differences in height between vegetation types cause spatially variable snow depth during winter, leading to spatially variable snow melt timing in spring, causing pronounced differences in topsoil mean temperature and temperature variability during those time periods. Summer topsoil temperatures were quite similar below most vegetation types, and not consistently related to active layer thickness at the end of August. The small-scale pattern of vegetation and its influence on snow cover height and snow melt governs the annual topsoil temperature in this permafrost-underlain landscape.

## 1 Introduction

15 Arctic ecosystems are changing rapidly, with widespread reports of air temperature increase (Stocker et al., 2013), shrinking snow cover (AMAP, 2011), and warming and degrading permafrost (Biskaborn et al., 2019). Permafrost thaw also depends on local influences on the transfer of heat into the ground including vegetation, hydrology, and soil physical properties. Connections between vegetation and soil thermal dynamics are critical for estimating the vulnerability of permafrost to thaw with continued climate warming and vegetation changes. Permafrost ecosystems are undergoing rapid vegetation change with in-  
20 creasing shrub abundance, cover, and biomass in many regions (Tape et al., 2006; Myers-Smith et al., 2011; Sturm et al., 2001; McManus et al., 2012; Lantz et al., 2013; Frost and Epstein, 2014). Yet, permafrost models and remote-sensing-driven monitoring approaches are still limited in their representation of small-scale spatial variability of snow and vegetation (Langer et al., 2013; Zhang et al., 2014; Park et al., 2016).



25 The interaction of vegetation and active layer thickness is very complex if the energy balance and soil properties are consid-  
ered simultaneously (Loranty et al., 2018). Observational evidence indicates that increased shrub cover reduces summer soil  
temperatures and decreases seasonal permafrost thaw depths (Anisimov et al., 2002; Walker et al., 2003, 2008; Blok et al.,  
2010), but tall shrub expansion in the tundra warms soils on annual timescales (Loranty and Goetz, 2012).

30 Zhang et al. (2018) found the largest offset between air and soil temperature in the low Arctic at an mean annual air tem-  
perature of roughly  $-10^{\circ}\text{C}$  due to snow cover and vegetation variability. In winter, snow insulates the soil from the cold air  
temperature. The resulting difference between the soil and air temperature is important for the ground thermal regime and thus  
permafrost temperatures (Zhang, 2005). This temperature difference varies widely in space, and how faithfully this parameter  
is represented differs widely in different land surface models (Wang et al., 2016). The insulating effect of snow is driven by  
snow depth, texture, and density, which are affected by snow redistribution and the formation of depth hoar (Zhang et al.,  
1996; Pomeroy et al., 1997). Vegetation affects snow depth and density because tall shrubs trap snow (Pomeroy et al., 2006;  
35 Sweet et al., 2014); also some vegetation types preferentially grow in locations with deeper snow cover in order to be protected  
from cold air temperatures (Sturm et al., 2005). This association leads to warm soil temperature in winter below tall shrubs  
(Lantz et al., 2009; Frost et al., 2018) and in tussock tundra which is commonly found in depressions (and experiences long  
freeze-back periods); in contrast, lichen tundra is usually associated with wind exposed hill tops and ridges which accumulate  
the least snow (Pomeroy et al., 1997; Burn and Kokelj, 2009).

40 Snow melt timing is considered one of the most important drivers of active layer thickness end of summer (Chapin et al.,  
2005; Wilcox et al., 2019). However, in certain areas the strong association may also be an artefact of the confounding relation-  
ship with other variables which strongly affect the active layer thickness. For instance, wind-blown ridges with thin snow cover  
and hence early snow melt also tend to store less organic matter, and are therefore less insulating, (Michaelson et al., 1996)  
than more sheltered locations where more snow is deposited. Also, depressions and tall shrub sites that accumulate deep snow  
45 cover and exhibit late snow melt are expected to be moister and to accumulate more peat and organic soil as compared to wind-  
exposed ridges (Walker et al., 2008). Therefore, the thicker moss and organic layer at tussock and tall shrub sites may be the  
factor that helps to keep the active layer cooler and shallower, rather than the late snow melt (Walker et al., 2008; Frost et al.,  
2013; Loranty et al., 2018). Summer surface temperature is influenced by vegetation through radiation shading and rainfall  
interception and evaporation (Loranty and Goetz, 2012; Zwieback et al., 2019). Tall vegetation cover is more closely coupled  
50 to increased soil organic matter (Pajunen et al., 2011) and decreased soil moisture during summer. These factors generally lead  
to reduced summer soil warming below tall shrubs (Frost et al., 2018) as less energy is available below the canopy and the  
soil tends to be drier and is thus more insulating. While these factors lead to reduced summer warming underneath shrubs, the  
magnitude and even the sign of this association varies in space and time. To exploit vegetation cover as a proxy for permafrost  
soil temperatures in summer, detailed observations of soil temperature and vegetation cover are required. The influence of all  
55 these factors on active layer thickness is complex and spatially variable, highlighting the difficulty of attributing active layer  
thickness trends to any one particular variable.

This study assesses the complex relationship between vegetation cover, snow, and active layer thickness and explores the  
local seasonal variability of the three components. We hypothesise that in winter the dependence of topsoil temperatures on



vegetation is largely shaped by the association of vegetation with snow depth, owing to the strong insulating effect of snow. Moreover, we expect that in summer tall vegetation cools the soil through shading and evapotranspiration. We also hypothesise that the timing of snow melt and accumulation will be a dominant control on topsoil temperature during spring and autumn, with snow melt being largely affected by interactions between vegetation and snow depth.

In the current study, we aim to quantify the topsoil temperature variability and elucidate the correlation between such variability and vegetation cover, thus improving our understanding of the feedback mechanisms. The results provide a basis for upscaling and modelling attempts and assess the potential of vegetation remote sensing for permafrost applications.

## 2 Methods

### 2.1 Field site, soil, and vegetation

The Trail Valley Creek research site is located at the tree line in the tundra-taiga transition zone 45 km north of Inuvik, Northwest Territories, Canada, east of the Mackenzie Delta (133.499 °E, 68.742 °N, Figure 1a). The mean annual air temperature

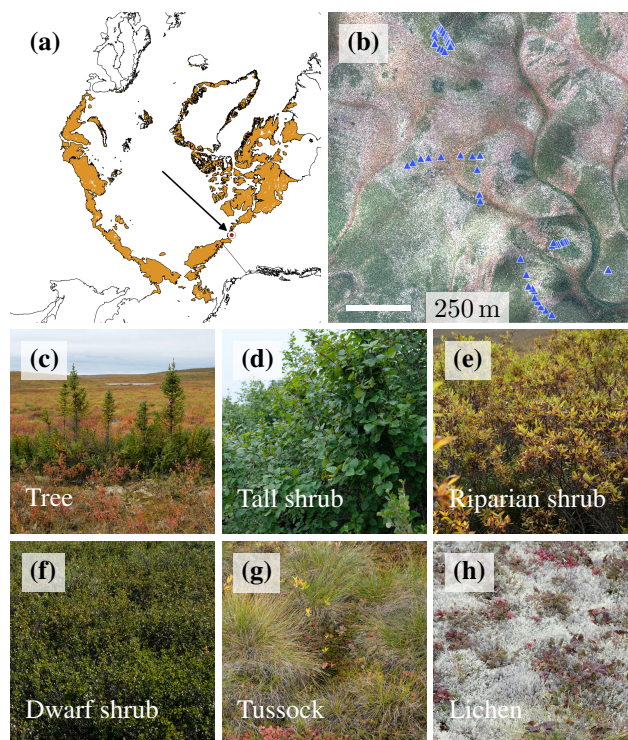


**Figure 1.** (a) Location of the Trail Valley Creek research station, Northwest Territories, Canada and Arctic tundra extent (data from Walker et al., 2005), (b) airborne orthophoto (Polar 5 airplane, MACS camera, 08/2018) of the site including topsoil temperature measurement locations, (c–h) six vegetation types used in this study.



70 in the 1999 – 2018 period was  $-7.9^{\circ}\text{C}$  (Environment and Climate Change Canada). During this 20-year period, it rose by  
1.1  $^{\circ}\text{C}$  per decade and the strongest warming trend was observed in May with an increase of 2.8  $^{\circ}\text{C}$  per decade (Environment  
and Climate Change Canada). The study site is underlain by continuous permafrost 100–150 m thick (Marsh et al., 2008) and  
is characterised by an active layer 25–100 cm deep at the end of summer. The catchment is dominated by mineral-earth hum-  
mocks which have a 5 cm thick organic layer and are underlain by fine grained material composed of roughly one third sand,  
75 one third silt, and one third clay (Quinton et al., 2000). Between the hummocks is a several decimeters thick peat layer, known  
as the inter-hummock zone (Quinton et al., 2000). The permafrost is ice-rich and thus susceptible to warming and thawing  
(Burn and Kokelj, 2009).

Gently rolling hills structure the lowland landscape (Marsh et al., 2010) and provide habitats for different tundra vegetation  
types and, in favourable locations, forest patches. The vegetation can be divided into six main types (Figure 1c–h) based on the  
80 classification by Walker et al. (2005):

- 1) **Trees** can be found in river channels and on adjacent slopes as well as in isolated patches. While trees growing in the forest  
patches can reach 10 m height, trees in isolated patches are usually 0.5–2.5 m tall (Anders et al., 2018). The tree species  
are white and black spruce (*Picea glauca* and *Picea mariana*) (Palmer et al., 2012). Forest patches cover roughly 2% of  
the landscape (Grünberg and Boike, 2019).
- 85 2) **Tall shrub** tundra is characterised by sparse patches of green alder (*Alnus alnobetula*) (Street et al., 2018); tall shrubs on  
hill slopes grow 3–5 m apart. While the alder shrubs are up to 2 m tall, the area between the shrubs is covered by shorter  
shrub species such as dwarf birch (*Betula glandulosa*) and by grasses and sedges. Tall shrubs (class S2 (low-shrub tundra)  
in Walker et al. (2005)) cover at least 11% of the wider Trail Valley Creek area (Grünberg and Boike, 2019).
- 3) **Riparian shrub** tundra can be found next to streams and at water tracks. Willow (*Salix*) species dominate these areas and  
90 grow up to 2.1 m tall. Additional shrub species include green alder and dwarf birch. Riparian shrubs (class S2 (low-shrub  
tundra) in Walker et al. (2005)) cover about 14% of the landscape (Grünberg and Boike, 2019).
- 4) **Dwarf shrub** tundra is one of the most abundant vegetation types growing on hill tops and slopes. In general, dwarf birch  
forms a dense canopy 20–50 cm high; in extreme cases it can reach 1 m. Dwarf birch is often complemented by shorter  
dwarf shrubs such as Labrador tea (*Ledum palustre*) and mountain cranberry (*Vaccinium vitis-idaea*), forbs (e.g. sweet  
95 coltsfoot, *Petasites frigidus*), graminoids, mosses, and lichen (Street et al., 2018). Dwarf shrubs (class S1 (erect dwarf-  
shrub tundra) in Walker et al. (2005)) cover roughly 24% of the landscape (Grünberg and Boike, 2019).
- 5) **Tussock** tundra is mostly located in flat, poorly drained areas. Tussock-forming sedges such as cotton grasses (*Eriophorum*)  
and *Carex* species dominate. However, a variety of dwarf shrubs such as dwarf birch, willows, Labrador tea, mountain  
cranberry, bilberry (*Vaccinium uliginosum*), crowberry (*Empetrum nigrum*), bearberry (*Arctostaphylos uva-ursi*), and  
100 cloudberry (*Rubus chamaemorus*) are also present and mosses can be found between the tussocks. The vegetation height  
is 10–30 cm in general. Tussock tundra (class G4 (tussock-sedge, dwarf-shrub, moss tundra) in Walker et al. (2005)) is  
the most abundant vegetation type in the study area with roughly 37% coverage (Grünberg and Boike, 2019).



105 **6) Lichen** tundra is dominated by lichen and dwarf shrubs 3–15 cm high, including mostly Labrador tea, mountain cranberry, crowberry, bearberry, and cloudberry. Some graminoids may also be present. Lichen tundra (class S1 (erect dwarf-shrub tundra) in Walker et al. (2005)) covers about 10% of the study area (Grünberg and Boike, 2019).

The approximate current spatial distribution of the six vegetation types and water is shown in Figure 2. The extent of tall shrub cover has expanded in the past and is likely to increase in the future at the Trail Valley Creek study site (MacKay, 1995; Lantz et al., 2010).

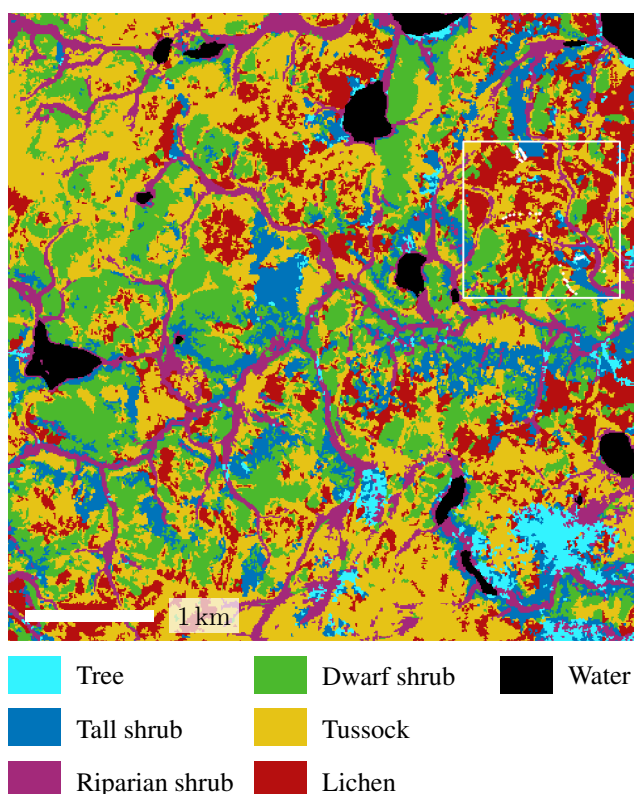


**Figure 2.** Vegetation map of the study region using the vegetation types as described above (Grünberg and Boike, 2019); the map is based on airborne orthophotos and vegetation height derived from airborne laser scanning (Anders et al., 2018); the white square indicates the study site extent including all sensor locations (white plus) as shown in Figure 1b.

## 2.2 Field measurements

110 Topsoil temperature was measured for two years at 68 locations distributed below different vegetation types at a maximum distance of 1200 m between the sensors in the study area (Figure 1b). We used iButton® temperature loggers (DS1922L) at 11 bit (0.0625 °C) resolution with an accuracy of 0.5 °C provided by the manufacturer. The sensors are 17 mm in diameter and 6 mm thick. Before deployment, we coated them with plastic to ensure water resistance. We tested all sensors in an ice bath



and verified the temperatures measured at the zero curtain. As all sensors had zero-curtain temperatures between  $-0.12^{\circ}\text{C}$  and  
115  $0.30^{\circ}\text{C}$ , we assume that the accuracy provided by the manufacturer is realistic.

We installed all temperature loggers as close as possible to the surface (soil, moss, or lichen) but deep enough to be protected  
from solar radiation (typically 1–3 cm deep). The measurement interval was every three hours, the measurement periods were  
27 August 2016, 17:00 (local time) to 03 September 2017, 08:00 and 04 September 2017, 05:00 to 22 August 2018, 14:00. In  
between the two measurement periods, the sensors had to be removed in order to obtain data records and were reinstalled at  
120 the same positions. We peeled off the coating, read out the data, and used tape as the new coating, as the plastic could not be  
reapplied in the field setting. This was done in the field to assure that each sensor was reinstalled as close as possible to the  
original location. However, the coating was different and possibly the micro-location and the contact to the surrounding moss,  
lichen or soil also differed slightly. Thus, we treated the two periods separately in our statistical analysis.

We classified the vegetation type into one of the six categories described above at each topsoil temperature location based  
125 on observations in the field and pictures taken while installing and removing the sensors. Maximum vegetation height was  
measured from 04–06 August 2019 within 30 cm around the sensor position.

Depth to the frozen soil was measured on 22 and 23 August 2018 three times around each topsoil temperature location within  
a 30 cm radius. We averaged the three values before continuing with the statistical analysis. Thawing of the soil potentially  
continues until freeze-back starts in October; thus, maximum thaw depths were not recorded. Snow depth was measured  
130 on 30 April 2017 approximately at the topsoil temperature locations based on a hand-held GPS because the flags marking  
each location were buried below the snow. In 2018, snow depth was measured by calculating the difference between a digital  
elevation model (DEM) of the snow and a DEM of the bare ground. The snow DEM was created using structure from motion  
photogrammetry in the software Pix4Dmapper (Pix4D SA, 2019), using images taken by an eBee Plus RTK at 3.5 cm/pixel  
resolution on 22 April 2018 (Mann, 2018). The 1 m resolution bare ground DEM was created using airborne LiDAR acquired  
135 in 2008 (Hopkinson et al., 2009). The resulting 1 m resolution snow depth raster was calibrated using 1370 Magnaprobe (Sturm  
and Holmgren, 2018) snow depth measurements taken between 19 and 25 April 2018.

### 2.3 Data analysis

Before analysis, we checked the quality of all time series data during the two measurement periods and removed the series if (a)  
the data record had more than 10% data gaps (4 series), (b) the mean deviation of topsoil temperature minus air temperature in  
140 summer was less than  $-5^{\circ}\text{C}$  indicating that the sensor was either buried too deep and affected by the permafrost or affected by  
running water (3 series), or (c) more than 5% of the single summer measurements were more than  $7^{\circ}\text{C}$  above air temperature  
indicating additional sensor warming by direct solar radiation (8 series) (Figure A1). We used air temperature measurements  
by Environment and Climate Change Canada at Trail Valley Creek for this comparison. The number of remaining data series  
in each measurement period per vegetation type is listed in Table 1.

145 The definition of seasons used in our statistical analysis is based on mean daily air temperatures of the last 20 years (1999–  
2018) at Trail Valley Creek (Environment and Climate Change Canada). To obtain a complete 20-year record, we gapfilled the  
Trail Valley Creek data using a piecewise linear regression with data from the climate stations in Inuvik, 45 km further south.



**Table 1.** Number of data series per vegetation type in each measurement period; period 1: 27 August 2016, 17:00 (local time) to 03 September 2017, 08:00 and period 2: 04 September 2017, 05:00 to 22 August 2018, 14:00.

Vegetation type	Number of data series	
	Period 1	Period 2
Tree	3	3
Tall shrub	17	15
Riparian shrub	2	2
Dwarf shrub	15	17
Tussock	14	14
Lichen	10	9
Total	61	60

Furthermore, we smoothed the average annual cycle using a 7-day moving window (Figure A2). We define winter as all days with average air temperature below  $-15^{\circ}\text{C}$  (06 November - 10 April) while summer is defined as air temperature above  $8^{\circ}\text{C}$  on average (10 June - 25 August). The periods in-between are defined as spring and autumn (Figure A2).

We calculated a variety of different characteristics for each topsoil temperature series, namely (I) the mean value for the whole year, each season, and each month, (II) the range of all three hourly values between the 10th and the 90th percentile for the whole year, each season, and each month, (III) the slope of a linear regression of all daily average values within each season, i.e. the rate of warming or cooling, (IV) the cumulative sum of positive degree days from the beginning of the melt season until the end of August, (V) the day of the year when the soil temperature first rose above  $-0.5^{\circ}\text{C}$  which indicates the beginning of the thawing period, (VI) the day of the year when the soil temperature first rose above  $0.5^{\circ}\text{C}$  which indicates the end of the thawing period, and (VII) the day of the year when the soil temperature first drops below  $-0.5^{\circ}\text{C}$  which indicates the end of the freezing period in autumn. We used  $-0.5^{\circ}\text{C}$  and  $0.5^{\circ}\text{C}$  as thresholds instead of  $0^{\circ}\text{C}$  to account for sensor uncertainty. We used Python 3.6 to analyse the topsoil temperature series. In boxplots, we always show the absolute minimum and maximum as whiskers, the 25th and 75th percentile as the box, and the median as a line within the box.

In terms of statistical analysis, we calculated Pearson's correlation coefficients for all numerical variables. To assess the relationship of vegetation type to topsoil temperature characteristics, active layer thickness, and snow depth, we used a linear model (lm in R) to estimate the adjusted  $R^2$  and the fraction of variance explained by vegetation type. Prior to the analysis, we excluded the vegetation types 'tree' and 'riparian shrub', as we do not have enough measurement series for these types. We assessed the impact of vegetation type on topsoil temperature characteristics based on all data series from both measurement periods. By analysing the two periods separately in the statistical model we accounted for the systematic differences between the years. For example, the summer of 2017 was warmer and started earlier than the summer of 2018. When we were interested in the impact of vegetation type on active layer thickness and snow depth, we used all sensor locations, even those, for which



we removed the temperature record, for example due to missing data. Results which were not significant at a level of 0.05 are  
170 shown in grey. We used R version 3.4 for all statistical analyses.

### 3 Results

We found a complex relationship between the different topsoil temperature characteristics, snow depth, active layer thickness, and vegetation in space. In general, the temperatures correlate well for all months between December and April (Figures 3 and 4). Locations which are colder in winter correspond to warmer topsoil temperatures in May; however, the correlation  
175 of May temperatures with winter temperatures is much stronger for the first period (September 2016 – August 2017) than for the second (September 2017 – August 2018). The summer temperatures between June and September are also highly correlated. In the first period, November topsoil temperature correlates well with October values and thus belongs to autumn, while November correlates more strongly with the winter months in the second period. Due to the long winter, the mean annual topsoil temperature correlates strongly with the topsoil temperature of the winter months, while it is almost uncorrelated with  
180 the summer topsoil temperature. The end date of the spring thawing period is strongly related to winter temperatures, snow depth and active layer thickness. Contrary to this, the date of thawing is not related to summer topsoil temperature (Figures 3 and 4).

The annual mean topsoil temperature recorded by all single sensors varies between  $-3.7^{\circ}\text{C}$  and  $-0.8^{\circ}\text{C}$  in the first period and between  $-3.7^{\circ}\text{C}$  and  $0.1^{\circ}\text{C}$  in the second period. In both periods, we find both the warmest and the coldest values in  
185 tussock tundra. On average, lichen tundra has the coldest topsoil temperature with  $-2.6^{\circ}\text{C}$  and  $-2.3^{\circ}\text{C}$  in the first and second period, respectively. The warmest average topsoil temperature of  $-2.0^{\circ}\text{C}$  and  $-1.3^{\circ}\text{C}$  in the first and second period were measured below tall shrubs. If we consider the approximate landscape fractions of each vegetation type (Section 2.1), we estimate a mean annual topsoil temperature of  $-2.3^{\circ}\text{C}$  and  $-1.7^{\circ}\text{C}$  in the first and second period, respectively.

#### 3.1 Soil temperature and vegetation in autumn

190 The two years 2016 and 2017 had different meteorological conditions in autumn. While air temperature dropped gradually to  $-7^{\circ}\text{C}$  before the first snowfall in 2016 (Figure B1a), daily mean air temperature had only dropped to  $0^{\circ}\text{C}$  by the date of the start of the snow accumulation in autumn 2017. Thus, the topsoil was significantly cooler in October 2016 as compared to 2017 (Figure 5d).

Autumn topsoil temperatures and cooling rates are not significantly related to vegetation type (Figure 5a–d, Table 2). The  
195 same is true for the start of the frozen period, which is almost identical at most sensor locations independent of vegetation type (Figure 5e). However, we observed considerable variability in the mean temperature within each vegetation type, at the landscape level, and between the different years. Considering the complete autumn season (26 August – 05 November), the mean autumn temperatures vary between  $-0.9^{\circ}\text{C}$  and  $1.2^{\circ}\text{C}$  in 2016 and between  $0.3^{\circ}\text{C}$  and  $1.7^{\circ}\text{C}$  in 2017. For October only, the range of mean topsoil temperatures was even higher, with a difference of  $4.3^{\circ}\text{C}$  and  $3.0^{\circ}\text{C}$  between the coldest and  
200 the warmest locations in 2016 and 2017, respectively (Figure 5d). Similar differences can be observed in the cooling rates,



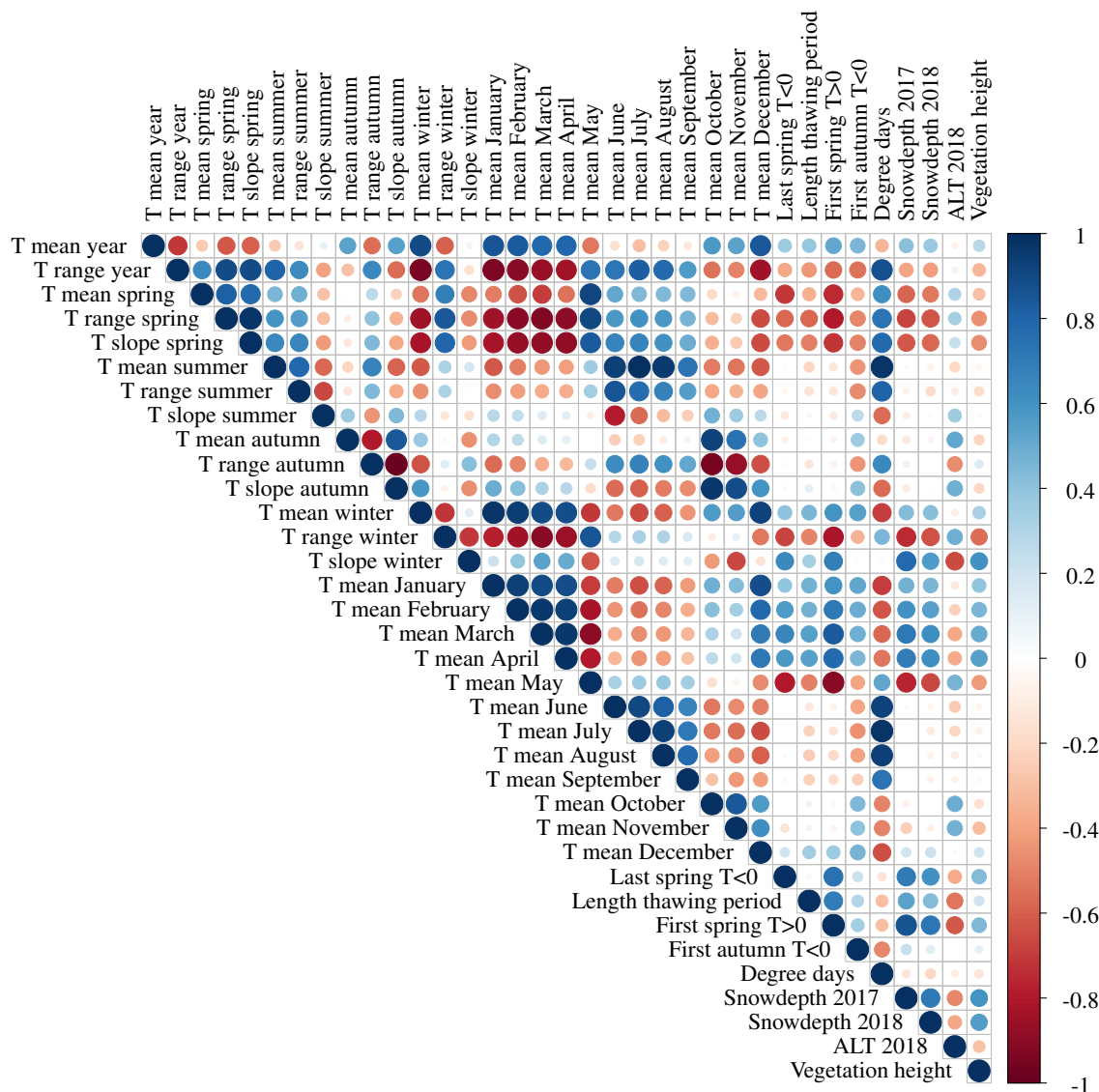


**Figure 3.** Pearson's correlation coefficients of all topsoil temperature characteristics ( $^{\circ}\text{C}$ ), active layer thickness (cm), and snow depth (cm) in the first period (September 2016 to August 2017).

which varied most strongly within tussock tundra and tall shrubs. Some locations within these two types cool down more than twice as fast as other locations (Figure 5c).

### 3.2 Soil temperature, snow, and vegetation in winter

There were significant differences in soil temperature between the two winter seasons (06 November - 10 April). Average topsoil temperatures were roughly  $2^{\circ}\text{C}$  colder beneath all vegetation types in the winter 2016/2017 as compared to the following

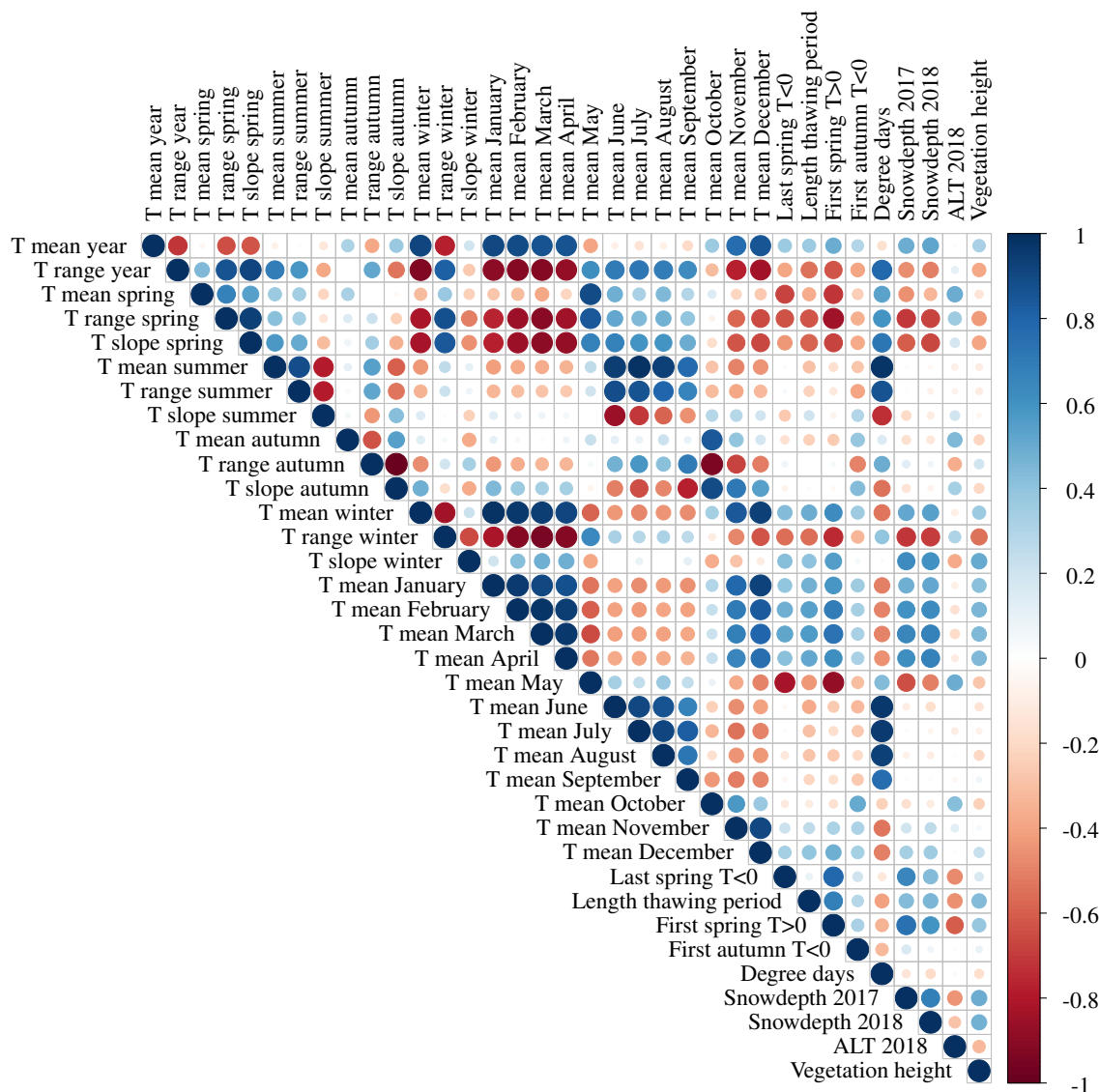


**Figure 4.** Pearson's correlation coefficients of all topsoil temperature characteristics ( $^{\circ}\text{C}$ ), active layer thickness (cm), and snow depth (cm) in the second period (September 2017 to August 2018).

year. This observation agrees well with the difference in mean winter air temperature of  $-20.3^{\circ}\text{C}$  and  $-18.2^{\circ}\text{C}$  in the first and second period, respectively (Figure B1a).

There is a strong relationship between vegetation type and topsoil temperature in winter. Topsoil under tall shrub tundra stays warmest, followed by topsoil beneath tussock, dwarf shrub, and lichen tundra (Figure 6). Vegetation type explains 36% of the topsoil temperature variations in the coldest month (March) in a single year and 43% of the cooling rate during winter (Table 2). The coldest mean temperatures are associated with the highest temperature variations below lichen tundra (Figure 6).

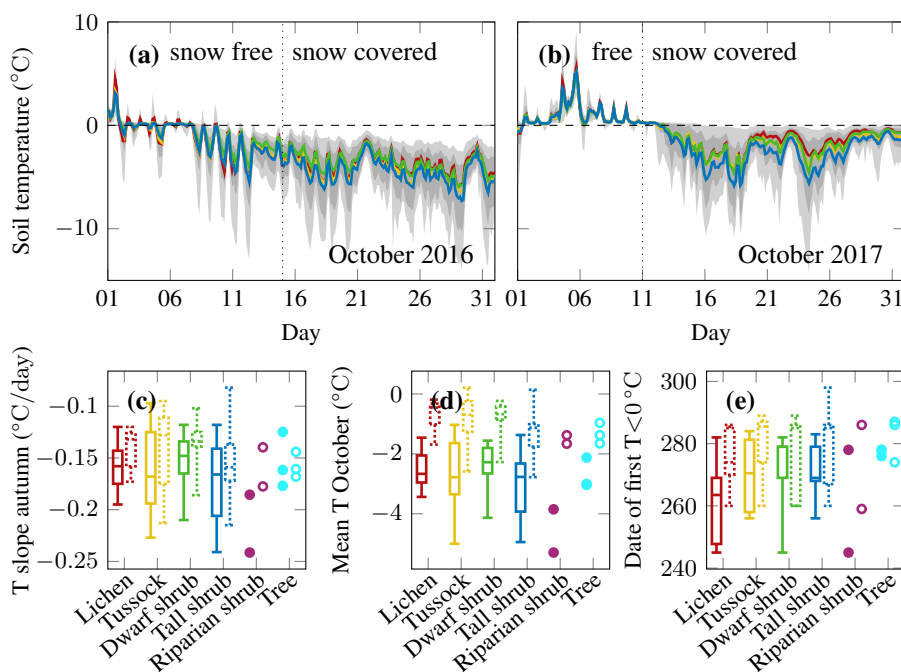


**Figure 5.** Topsoil temperature series of (a) October 2016 and (b) October 2017 representing autumn of the two different measurement periods; mean of all measurements below four different vegetation types in colour, the range of all single sensors in light grey and the range of all sensors between the 10th and 90th percentile in darker grey; the beginning of snow accumulation was derived from the Trail Valley Creek weather station albedo data; boxplots of all measurements per vegetation type with boxes of the first period left and the second period right and dotted; for riparian shrubs and trees all single observations are shown with filled symbols for the first period and open symbols for the second; (c) rate of cooling in autumn; (d) mean October topsoil temperature; (e) date when the freezing is completed.

Snow depth strongly mediates the association between vegetation type and winter soil temperatures. Different vegetation types show characteristic snow depth values (Figure 7a, f). The deepest snow cover is associated with tall shrubs, followed by tussock tundra and dwarf shrubs while lichen tundra is characterised by the shallowest snow cover. Vegetation explains 70% and 58% of the observed snow depth variability in 2017 and 2018, respectively (Table 2).

Several winter and spring topsoil temperature characteristics are also very strongly related to snow cover, in particular the day of the year when the topsoil warms above 0 °C, the topsoil temperature slope during winter cooling, and the mean temperature of the winter and spring months (Figure 7). In 2018, snow depth was less strongly related to vegetation or topsoil temperature characteristics than in 2017 (Figure 7, bottom row).

The predictability of snow depth from vegetation type is limited by the differences in snow cover in different years. For example, the snow depth at the end of April 2017 reached higher maximum and lower minimum values as compared to 2018 indicating a stronger snow redistribution. The correlation between snow depth values of the different years is  $R^2 = 0.49$  (Figure 8).



**Table 2.** Relationship of vegetation and topsoil temperature characteristics, active layer thickness, snow depth, and vegetation height expressed by the fraction of variance explained by vegetation type in a statistical model ( $\ln(\text{response} \sim \text{period} + \text{vegetation type})$ ) and the adjusted  $R^2$ ; complete data set accounting for the measurement period of topsoil temperature first; results which are not significant at a level of 0.05 are shown in grey.

Response	Fraction of variance	Adjusted $R^2$
Mean annual T ( $^{\circ}\text{C}$ )	0.125	0.25
Date of first $T > 0^{\circ}\text{C}$	0.548	0.55
Cumulative degree days ( $^{\circ}\text{C}$ )	0.071	0.56
Mean T May ( $^{\circ}\text{C}$ )	0.543	0.53
Mean T July ( $^{\circ}\text{C}$ )	0.118	0.10
Mean T October ( $^{\circ}\text{C}$ )	0.035	0.51
Mean T March ( $^{\circ}\text{C}$ )	0.355	0.56
T slope spring ( $^{\circ}\text{C}/\text{day}$ )	0.327	0.40
T slope summer ( $^{\circ}\text{C}/\text{day}$ )	0.058	0.51
T slope autumn ( $^{\circ}\text{C}/\text{day}$ )	0.053	0.09
T slope winter ( $^{\circ}\text{C}/\text{day}$ )	0.432	0.56
Active layer thickness 2018 (cm)	0.342	0.31
Snow depth 2017 (cm)	0.699	0.68
Snow depth 2018 (cm)	0.584	0.56
Vegetation height (cm)	0.427	0.40

### 3.3 Soil temperature, snow, and vegetation in spring

225 Starting from the beginning of May, the relationship between vegetation and topsoil temperature is opposite to that found in  
winter (Figure 9a, b). In general, topsoil temperatures beneath all vegetation types are very similar in the last few days of April.  
The soil below lichen tundra warms up first and most strongly and shows the most pronounced diel variation. Dwarf shrub  
tundra is still cooler in May and warms up a bit more slowly than lichen tundra. Tussock tundra topsoil temperatures rise above  
0  $^{\circ}\text{C}$  even later; tall shrub temperatures were the last to reach positive temperatures in 2017 and were similar to tussock tundra  
230 in 2018. This order becomes apparent in the slope of spring temperatures, in the mean May temperatures, and in the day of  
the year when the thawing period ends (Figure 9c–e). Using a statistical model, we find that vegetation type explains 54% of  
the observed variability in the end of the thaw date and the mean May temperature and 33% of the variability in the spring  
warming rate (Table 2).

Furthermore, snow melt timing is different between the years. Our observations of topsoil temperature indicate that the snow  
235 melt period of the entire landscape was 20 and 40 days long in 2017 and 2018, respectively (Figure 9e). This observation

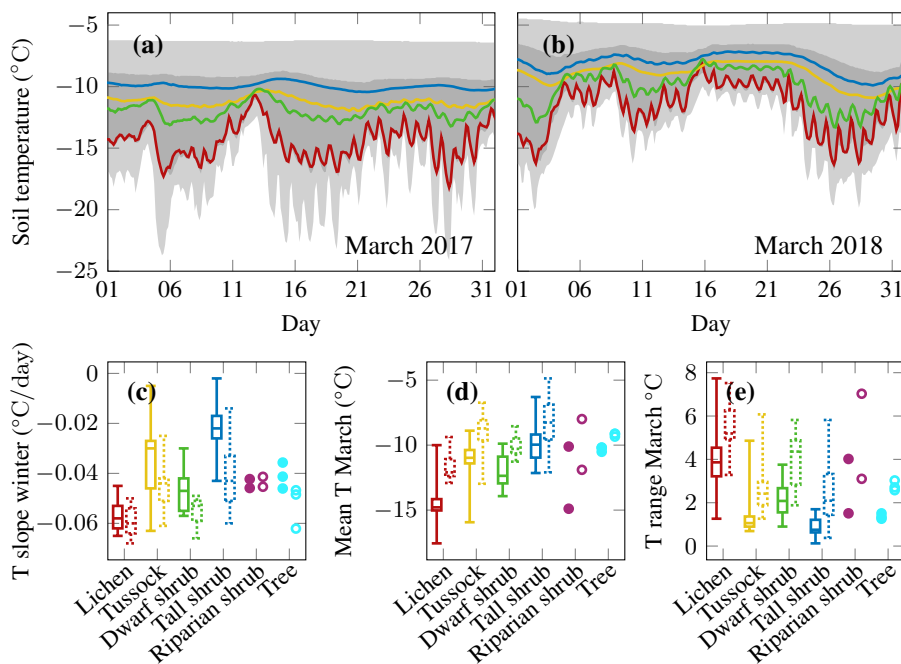


**Figure 6.** Topsoil temperature series of (a) March 2017 and (b) March 2018 representing the coldest topsoil temperatures in winter of the two different measurement periods; the mean of all measurements below four different vegetation types is shown in colour, the range of all single sensors is shown in light grey, and the range of all sensors between the 10th and 90th percentile is shown in darker grey; boxplots of all measurements per vegetation type are shown with boxes of the first period on the left and boxes representing the second period on the right and dotted; all single observations for riparian shrubs and trees are shown by filled symbols for the first period and open symbols for the second; (c) rate of cooling in winter; (d) mean March temperature; (e) range of March temperature.

is in contrast to the more spatially variable snow distribution observed in 2017 (Figure 8). The long melt period in 2018 is associated with a 3.4 °C colder mean May air temperature and more cold spells as compared to May 2017 (Environment and Climate Change Canada) (Figure B1). However, due to the differences in snow melt timing, the cold May air temperatures in 2018 did not necessarily translate into cold topsoil temperatures. While lichen tundra measurements indeed reveal colder May topsoil temperatures in 2018, both years are similar for dwarf shrub soil and May 2018 is associated with later warmer topsoil temperatures below tussock tundra and tall shrubs.

### 3.4 Soil temperature, active layer thickness, and vegetation in summer

Topsoil temperatures in summer are more similar for all vegetation types than spring or winter temperatures (Figure 10a, b). In summer 2017, dwarf shrub tundra had the coolest summer temperatures. The other three vegetation types (excluding tree/riparian shrub) have almost identical mean values and the distributions largely overlap (Figure 10c, d). In 2018, the difference between dwarf shrubs and the other vegetation types was much smaller and the mean summer slope is almost equal for

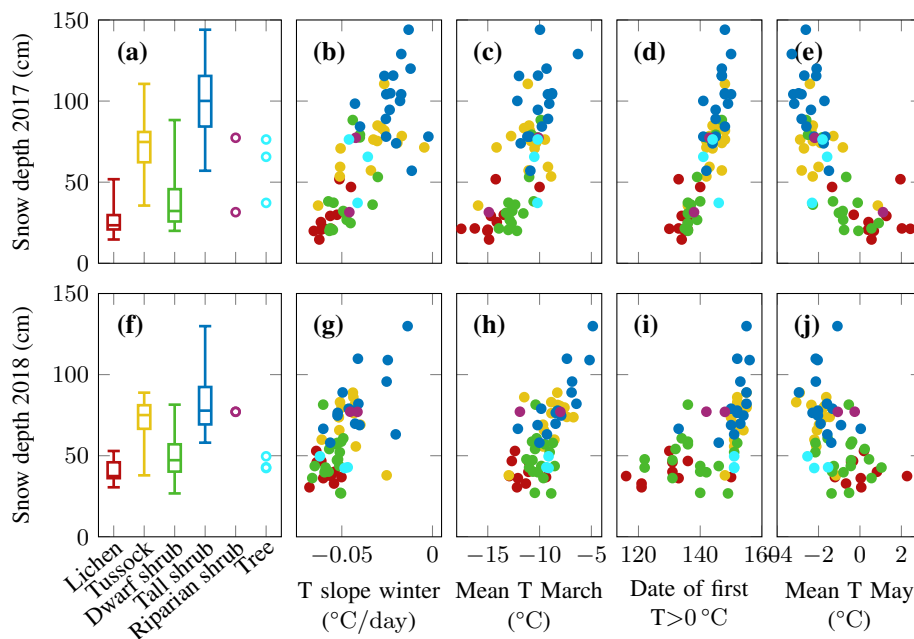


**Figure 7.** The relationship between snow depth end of April 2017 (top row) and 2018 (bottom row) and (a, f) vegetation type; (b, g) rate of cooling in winter; (c, h) mean temperature in March; (d, i) day of year when the topsoil warms above 0 °C; (e, j) mean temperature in May.

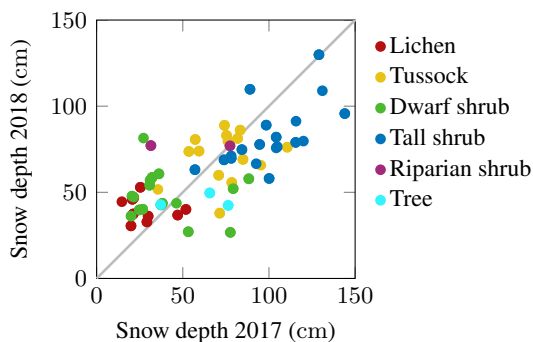


**Figure 8.** Snow depth measured at the end of April in 2017 and 2018 at approximately the same locations.

lichen, dwarf shrub, and tall shrub tundra, while tussock tundra warmed at a slightly lower rate. The temperature difference between the two years is much larger than the variability between vegetation types. The 2018 mean summer air temperature was 2.7 °C cooler than in 2017. This difference translates into topsoil temperatures which are, on average per vegetation type, 1.3–2.2 °C colder in 2018, with the smallest difference for dwarf shrubs. The small difference between vegetation types is also reflected in the low fraction of July mean temperature variance (12%) that can be explained by the vegetation type (Table 2). Lichen tundra featured slightly higher cumulative degree days than the other three vegetation types, which all showed sim-

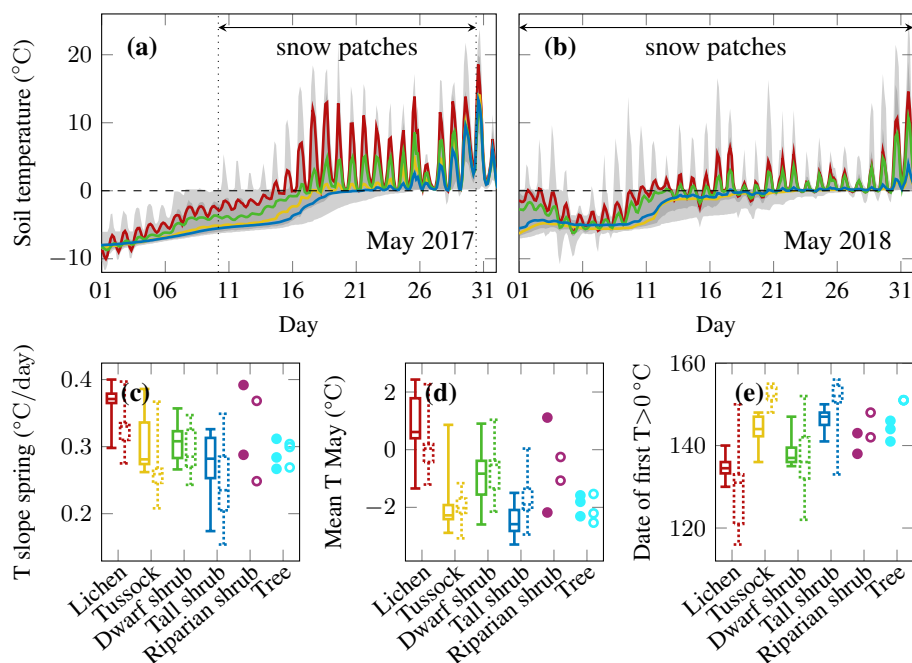


**Figure 9.** Topsoil temperature series of (a) May 2017 and (b) May 2018 representing spring of the two different measurement periods; mean of all measurements below four different vegetation types is shown in colour, the range of all single sensors is shown in light grey, and the range of all sensors between the 10th and 90th percentile is shown in darker grey; boxplots of all measurements per vegetation type are represented by boxes of the first period on the left and the second period on the right and dotted; for riparian shrubs and trees all single observations are shown with filled symbols for the first period and open symbols for the second; (c) rate of warming in spring; (d) mean May temperature; (e) date when thawing is complete.

ilar values on average (Figure 10e). Even though the influence of vegetation type on cumulative degree days is statistically significant, vegetation only explains 7% of the observed variability (Table 2).

255 There is a weak association between active layer thickness and vegetation type. On average, we found deeper active layers below lichen and dwarf shrub tundra as compared to tussock and tall shrub tundra (Figure 11a). The variability in active layer thickness within each vegetation type was substantial. Correspondingly, vegetation was only weakly related to active layer thickness at the end of summer as it explains only 34% of the variability between different locations (Table 2).

In terms of topsoil temperature characteristics, active layer thickness is most strongly related to the date when the topsoil  
 260 temperature first rises above 0 °C in spring (Figure 11d). While a moderate association exists with other spring and winter characteristics, such as the cooling rate in winter (Figure 11c), summer characteristics show no significant correlation with active layer thickness when all measurements are considered (Figure 11e). However, when we consider only the dwarf shrub locations, sensors with higher degree days are associated with deeper active layers (Figure 11e). Deep active layers are also associated with higher topsoil temperatures in October (Figure 4). Within vegetation types, the thawing degree day correlation  
 265 is very weak for tall shrubs (and other types), and so is the date of the first T>0. Conversely, the date of the first T>0 also

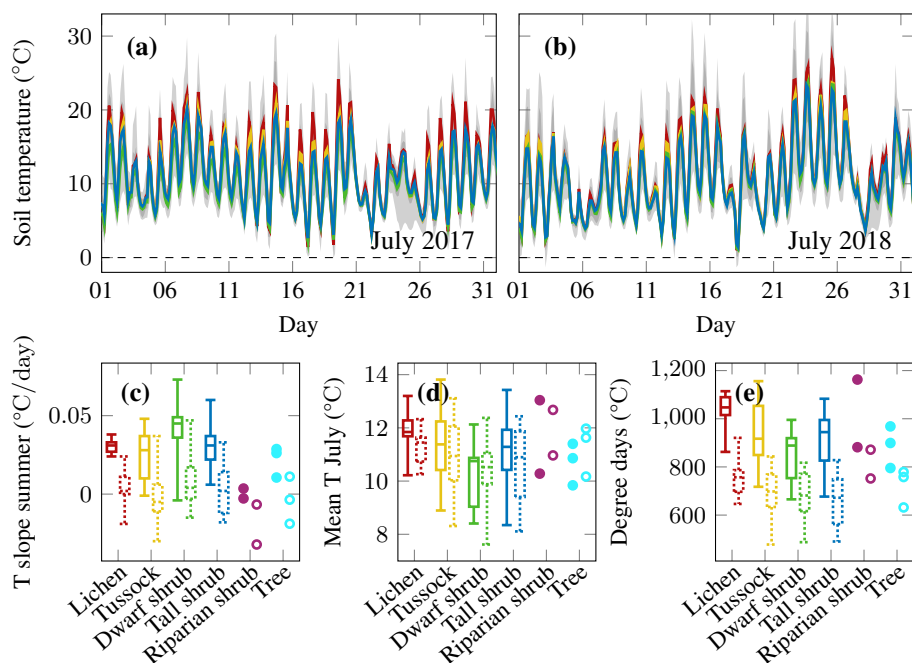


**Figure 10.** Topsoil temperature series of (a) July 2017 and (b) July 2018 representing summer of the two different measurement periods; mean of all measurements below the four different vegetation types is shown in colour, the range of all single sensors is shown in light grey, and the range of all sensors between the 10th and 90th percentile is shown in darker grey; boxplots show all measurements per vegetation type with boxes of the first period on the left and the second period on the right and dotted; for riparian shrubs and trees all single observations are shown with filled symbols for the first period and open symbols for the second; (c) rate of warming in summer; (d) mean July temperature; (e) cumulative sum of positive degree days until the end of August.

apparently explains a moderate fraction of the active layer thickness variance within lichen and dwarf shrub tundra. For tall shrubs, we can observe that warmer winter temperatures are associated with deeper active layers (Figure 11b).

#### 4 Discussion

In this study, we analysed how local variability of vegetation cover relates to topsoil temperature, active layer thickness and snow depth at one site at the Arctic forest–tundra transition. Both the observed variability and the absolute values are site dependent.

In agreement with Kropp et al. (2020) we found that winter topsoil temperatures controlled annual mean temperatures, and that topsoil below tussocks and tall shrub tundra was generally warmer than topsoil below short-statured vegetation. Furthermore, we found that topsoil temperature was most variable under the snow cover in winter and during snow melt in May, while the spatial variability was less pronounced in summer and autumn, which agrees well with Gislén et al. (2014).



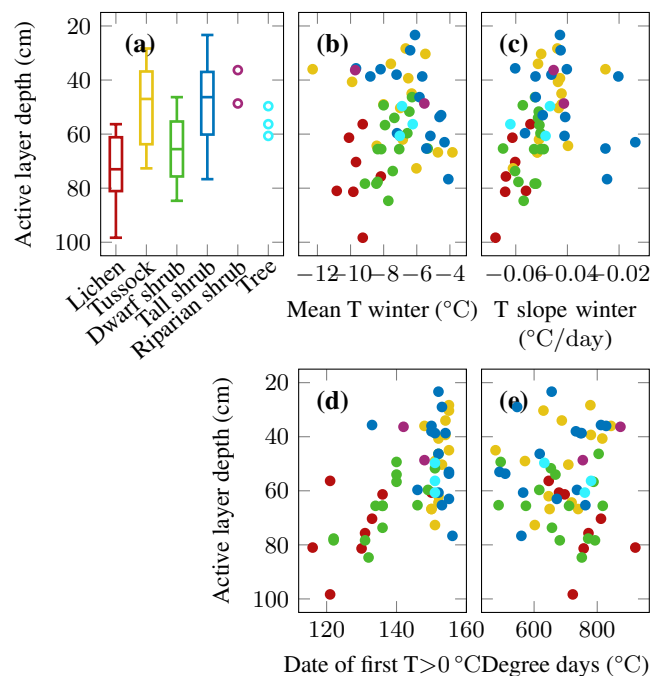


**Figure 11.** The relationship between active layer thickness at the end of August 2018 and (a) vegetation type; (b) mean topsoil winter temperature; (c) rate of topsoil cooling in winter; (d) day of the year when the topsoil warms above 0 °C; (e) cumulative sum of positive degree days until the end of August of the same year.

#### 4.1 Vegetation and soil temperature in relation to autumn processes

While vegetation type did not play a significant part in the autumn topsoil temperature variation, we found that at all locations the general pattern was dominated by air temperature and snowfall timing. However, we observed considerable variability between different locations and years. This variability is potentially driven by the soil cover of mosses or lichen, soil moisture, and microtopography rather than vascular plants.

#### 4.2 Vegetation and soil temperature in relation to winter snow processes

In winter, warm soil temperatures can be expected at locations with more snow such as below tall shrubs and in poorly drained and somewhat sheltered tussock-dominated areas (Lantz et al., 2009; Frost et al., 2018). The snow observed at our measurement locations was indeed deepest in tall-shrub areas, where soils were also the warmest in winter (Figure 7a, f). Across all vegetation types, the differences in snow depth influenced the winter topsoil temperatures, temperature variability, and cooling rates. Winter temperatures were coldest and most variable at vegetation types associated with low snow, in particular below lichen tundra and, to a lesser extent, below dwarf shrubs (Figure 6).



The variability of snow depth within vegetation types (Figure 7a, f) is likely due to (I) topography and microtopography influencing the deposition of blowing snow, (II) vegetation height and density differences within one vegetation type and (III) factors other than snow limiting shrub growth such as poor soil, too much or too little soil moisture, disturbances, and slow colonisation.

We also observed variability in the relationship between snow depth and winter topsoil temperature characteristics such as the soil cooling rate and the mean and range of temperature values in the winter months (Figure 7b, c, g, h). The topography of the site is gentle and cannot account for major differences in cold-season insolation; therefore, the variability is likely largely due to differences in snow density and texture. Differences in snow density and texture across the landscape can be caused by snow compaction at wind exposed sites, by loose snow accumulating within shrub canopies, and by the formation of depth hoar. We do not have detailed snow observations at our measurement locations to analyse such differences in detail. However, our results suggest that, for the same snow depth, topsoil temperatures in March are colder at lichen sites as compared to dwarf shrub sites (Figure 7c, h). This agrees very well with the observation that lichen tundra can be found at the most wind-exposed ridges. While historical surveys of snow density did not find differences between lichen and dwarf shrub tundra at the site ( $0.22 \text{ g cm}^{-3}$ , Wilcox et al. (2019)), snow texture and depth hoar formation likely differed between shrub and shrub-free areas (Belke-Brea et al., 2020), leading to differences in the heat conductivity of each snowpack.

#### 4.3 Vegetation and soil temperature in relation to spring processes

In spring, a thick snow cover delays soil warming and thus results in a reversal of the topsoil temperature – vegetation type relationship. We observed similar topsoil temperatures beneath all vegetation types in the last few days of April. The soil below tall shrubs was coldest in May, followed by the temperatures below tussocks and dwarf shrubs, while lichen tundra topsoil was already the warmest (Figure 9d).

We found that the date when the topsoil warmed above  $0^\circ\text{C}$  was strongly related to vegetation type in 2017, and less so in 2018 (Figure 9e). A strong relationship can be expected due to the influence of vegetation on snow depth, snow density, and snow melt energetics (Pomeroy et al., 2006; Wilcox et al., 2019). The weaker relationship in 2018 is likely due to the more complex spring weather patterns including multiple periods of warming and subsequent freezing periods.

In general the presence of shrubs enhances snow melt as soon as branches stick out of the snow, thus reducing surface albedo (Pomeroy et al., 2006; Marsh et al., 2010). Wilcox et al. (2019) made extensive measurements of snow-free date with a drone at the same study site in 2016 and showed that dwarf shrub areas become snow free earlier than non-shrub areas, regardless of snow depth and hillslope aspect. However, we did not observe this relationship at our locations, likely due to the small number of points we measured at compared to Wilcox et al. (2019). Instead, we found the topsoil warmed above  $0^\circ\text{C}$  first at the lichen tundra locations, even though they were similar in snow depth to the dwarf shrub locations (Figure 7d, i).

#### 4.4 Vegetation and soil temperature in relation to summer processes and active layer thickness

Although shrubs may reduce summer soil warming through shading and evapotranspiration (Frost et al., 2018), in our study, the summer difference between all vegetation types is very small, and shrub tundra is comparable to tussock tundra in terms



of topsoil temperature (Figure 10 and B2). Lichen tundra topsoil warms up slightly more, in particular during mid-day, but the average difference is less than 1 °C.

These generally small differences in topsoil temperature likely contribute to the weak relation between vegetation type and summer temperature characteristics (Figure 11a, e, Table 2). On the other hand, winter and spring temperature characteristics such as the date when the topsoil warmed above 0 °C, are strongly related to active layer thickness (Figure 11). The strong influence of snow-free date on active layer thickness has been highlighted in several other studies (Chapin et al., 2005; Wilcox et al., 2019). At first glance, our data suggest that the snow-free date and thus the length of the summer period is the most important driver for active layer thickness, while a warm winter temperature is unexpectedly associated with a shallow active layer (Figure 11b, d). However, this may be an artefact of the spatial correlation between snow depth and soil properties (Lorantý et al., 2018). For instance, both snow depth and organic layer thickness tend to be shallow on exposed lichen-covered ridges, and the latter favours deeper active layers. If we consider single vegetation types with presumably more uniform soil conditions, the importance of snow melt timing is strongly reduced. In particular, for tall shrubs and tussocks warm winter temperatures are related to deep active layers (Figure 11b) while the relationship with snow melt timing is weak for these two types (Figure 11d). It should also be noted that it was not recorded whether active layer thickness measurements were taken in a hummock or inter-hummock zone, which due to their vastly different soil properties, have a stronger effect on active layer thickness than any other variable (Wilcox et al., 2019). This reduces our ability to draw inferences from our active layer thickness measurements.

Vegetation type is thus a useful proxy for predicting topsoil temperatures in winter, through its modification of snowpack height, density, and texture. Conversely, its predictive value in summer is poor. The generally weak relationship between vegetation type and active layer thickness we found in our study hinders upscaling approaches such as in Nelson et al. (1997); Widhalm et al. (2017). This is likely related to variable soil thermal properties, as one would expect a strong relation between thawing degree days and active layer thickness for uniform soil properties. This is not the case at our site across vegetation types, echoing previous findings by (Nelson et al., 1997). Within dwarf shrubs, where more uniform soil properties may be expected, larger cumulative positive degree days are indeed associated with deeper active layers. Again, as we did not record whether active layer thickness measurements were made in hummocks or inter-hummock zones, a large portion of the variance remains unexplained. In summary, our observations suggest that vegetation type is a better predictor of the near-surface thermal regime in winter than in summer in the low Arctic.

## 5 Conclusions

Based on topsoil temperature data from 68 sensors at a low Arctic tundra site, we found large small-scale variability within and between vegetation types as well as between years and seasons. Autumn topsoil temperatures were dominated by atmospheric forcing and only weakly related to vegetation type. Conversely, vegetation type explained approximately one half of the variability in winter and spring soil temperature. An even stronger relation was observed between vegetation type and end-of-winter snow depth. Snow depth and, most likely, snow structural differences in space lead to pronounced differences in topsoil



mean temperature and temperature variability in the winter and spring months and in snow melt timing, all of which were  
355 strongly related to vegetation type. Summer topsoil temperatures were less variable in space, similar below most vegetation  
types, and not significantly related to active layer thickness at the end of August. At the landscape scale, we found that active  
layer thickness was most strongly related to snow melt timing. However, if we considered only specific vegetation types with  
presumably more similar soil conditions, mean winter temperature and summer thawing degree days played a more important  
part. The spatial variation of the mean annual soil temperature was dominated by the winter signal. To conclude, vegetation  
360 can, with limitations, be used as a proxy for snow depth variability at the local scale, but it is a poor proxy for summer and  
autumn topsoil temperature or active layer thickness.

## Appendix A: Methods

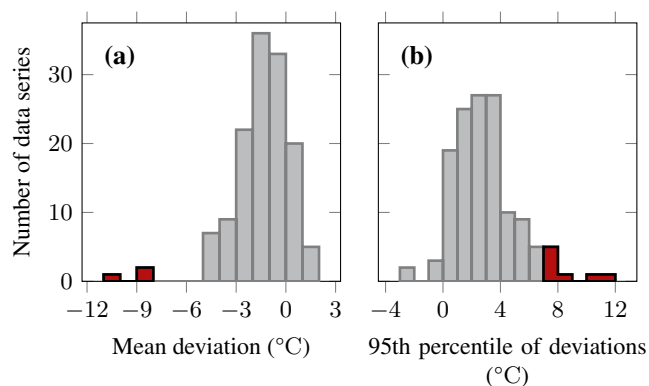


**Figure A1.** Histograms of the deviation of topsoil temperature minus air temperature in summer; (a) mean and (b) 95th percentile of the deviations for each sensor in each measurement period; data series coloured in red were removed from the analysis because (a) the average deviation was less than  $-5^{\circ}\text{C}$  indicating that the sensor was either buried too deep and affected by the permafrost or affected by running water (3 series) or (b) more than 5% of the single summer measurements were more than  $7^{\circ}\text{C}$  above air temperature indicating additional sensor warming by direct solar radiation (8 series); air temperature data by Environment and Climate Change Canada.

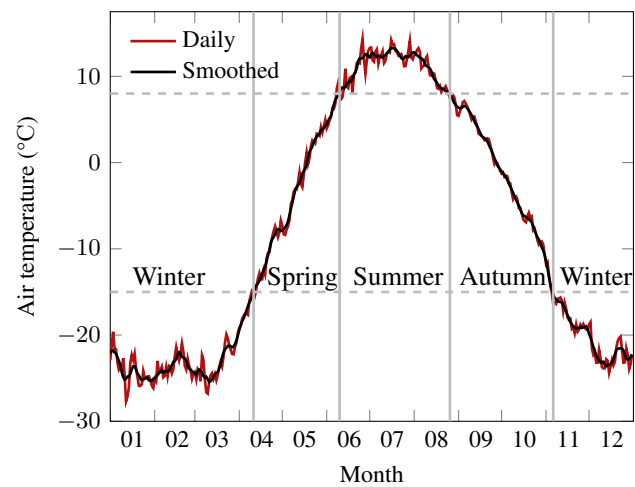


**Figure A2.** Mean annual cycle of air temperature at Trail Valley Creek for 1999–2018, gap-filled data series; daily values and values smoothed with a seven-day moving window as used for definition of the seasons; data by Environment and Climate Change Canada.

## Appendix B: Results

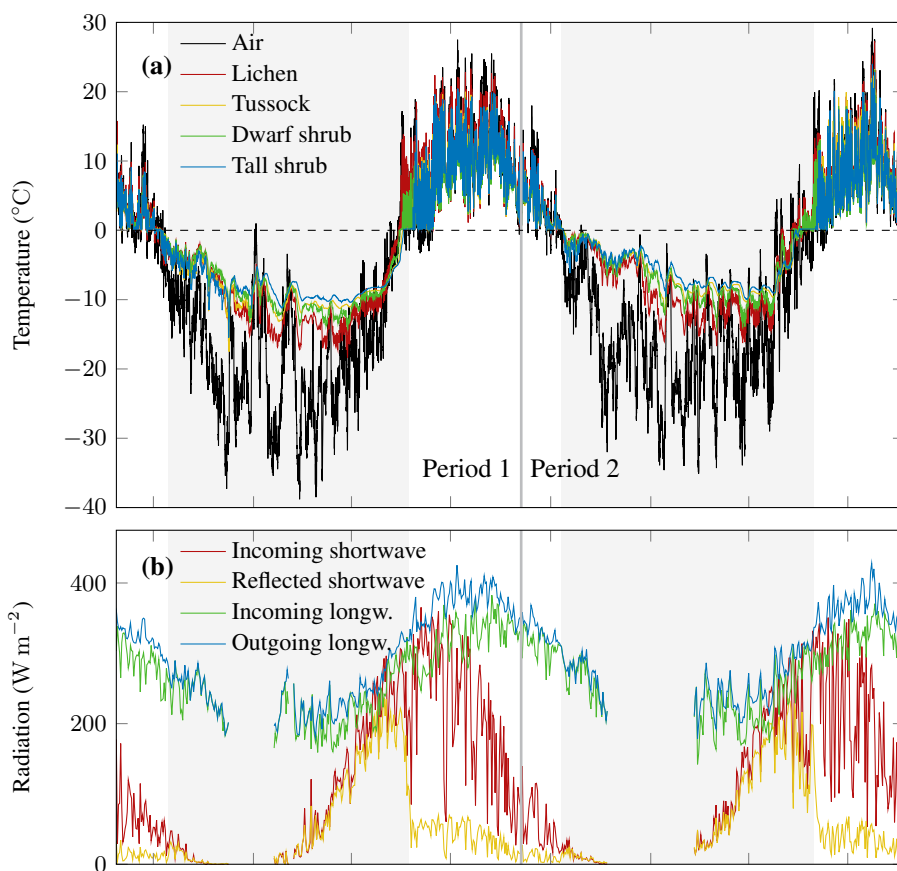


**Figure B1.** Meteorological conditions at the Trail Valley Creek weather station during the two study periods including snow cover estimated from daily albedo > 0.4 indicated as shaded area. (a) Air temperature by Environment and Climate Change Canada and median topsoil temperature of each vegetation type; (b) daily mean values of four component radiation.

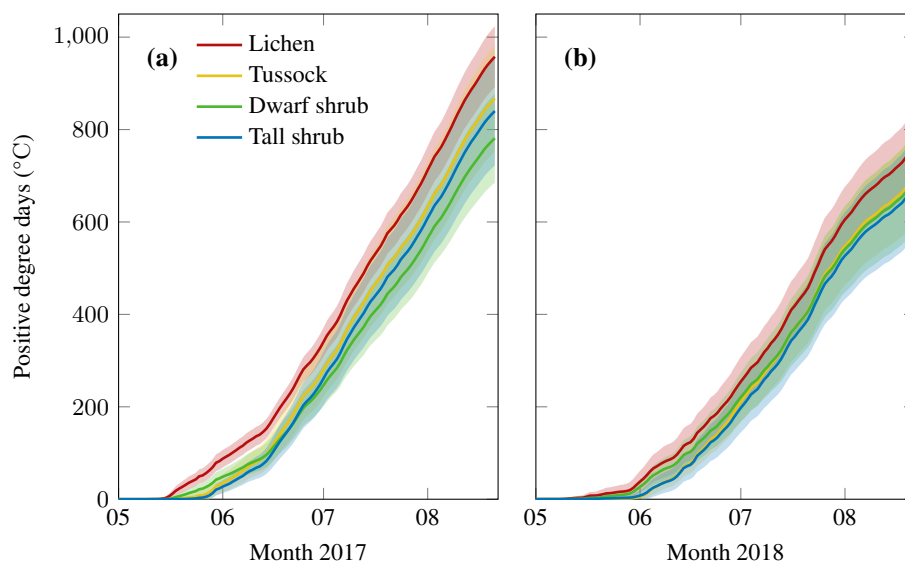


**Figure B2.** Cumulative positive degree days of topsoil temperature below different vegetation types; the lines indicate the mean of all series per type, the shaded areas represent the mean plus/minus the standard deviation; (a) 2017, (b) 2018.



*Author contributions.* J. Boike and I. Grünberg conceived the study. J. Boike, S. Zwieback, E. Wilcox, I. Grünberg, and several helpers  
365 carried out the field measurements. I. Grünberg analysed the data with input from J. Boike, E. Wilcox, and S. Zwieback. I. Grünberg  
prepared the manuscript with contributions from all co-authors.

*Competing interests.* We declare that no competing interests are present.

*Acknowledgements.* This contribution was financially supported by Geo.X, the Research Network for Geosciences in Berlin and Potsdam  
(Grant-number: SO 087 GeoX) and by funding from the Helmholtz Association in the framework of MOSES (Modular Observation Solutions  
370 for Earth Systems). We thank Cory Wallace, Branden Walker, Bill Cable, and Stephan Lange for helping with the data collection in the field.





## References

- AMAP: Snow, Water, Ice and Permafrost in the Arctic (SWIPA), Tech. rep., AMAP, <http://amap.no/swipa/>, 2011.
- Anders, K., Antonova, S., Boike, J., Gehrman, M., Hartmann, J., Helm, V., Höfle, B., Marsh, P., Marx, S., and Sachs, T.: Airborne Laser Scanning (ALS) Point Clouds of Trail Valley Creek, NWT, Canada (2016), <https://doi.org/10.1594/PANGAEA.894884>, 2018.
- 375 Anisimov, O. A., Shiklomanov, N. I., and Nelson, F. E.: Variability of seasonal thaw depth in permafrost regions: a stochastic modeling approach, *Ecological Modelling*, 153, 217–227, [https://doi.org/10.1016/S0304-3800\(02\)00016-9](https://doi.org/10.1016/S0304-3800(02)00016-9), 2002.
- Belke-Brea, M., Domine, F., Barrere, M., Picard, G., and Arnaud, L.: Impact of Shrubs on Winter Surface Albedo and Snow Specific Surface Area at a Low Arctic Site: In Situ Measurements and Simulations, *Journal of Climate*, 33, 597–609, <https://doi.org/10.1175/JCLI-D-19-0318.1>, 2020.
- 380 Biskaborn, B. K., Smith, S. L., Noetzli, J., Matthes, H., Vieira, G., Streletskiy, D. A., Schoeneich, P., Romanovsky, V. E., Lewkowicz, A. G., Abramov, A., Allard, M., Boike, J., Cable, W. L., Christiansen, H. H., Delaloye, R., Diekmann, B., Drozdov, D., Etzelmüller, B., Grosse, G., Guglielmin, M., Ingeman-Nielsen, T., Isaksen, K., Ishikawa, M., Johansson, M., Johannsson, H., Joo, A., Kaverin, D., Kholodov, A., Konstantinov, P., Kröger, T., Lambiel, C., Lanckman, J.-P., Luo, D., Malkova, G., Meiklejohn, I., Moskalenko, N., Oliva, M., Phillips, M., Ramos, M., Sannel, A. B. K., Sergeev, D., Seybold, C., Skryabin, P., Vasiliev, A., Wu, Q., Yoshikawa, K., Zheleznyak, M., and Lantuit,
- 385 H.: Permafrost is warming at a global scale, *Nature Communications*, 10, 2041–1723, <https://doi.org/10.1038/s41467-018-08240-4>, 2019.
- Blok, D., Heijmans, M. M. P. D., Schaepman-Strub, G., Kononov, A. V., Maximov, T. C., and Berendse, F.: Shrub expansion may reduce summer permafrost thaw in Siberian tundra, *Global Change Biology*, 16, 1296–1305, <https://doi.org/10.1111/j.1365-2486.2009.02110.x>, 2010.
- Burn, C. R. and Kokelj, S. V.: The environment and permafrost of the Mackenzie Delta area, *Permafrost and Periglacial Processes*, 20,
- 390 83–105, <https://doi.org/10.1002/ppp.655>, 2009.
- Chapin, III, F. S., Sturm, M., Serreze, M. C., McFadden, J. P., Key, J. R., Lloyd, A. H., McGuire, A. D., Rupp, T. S., Lynch, A. H., Schimel, J. P., Beringer, J., Chapman, W. L., Epstein, H. E., Euskirchen, E. S., Hinzman, L. D., Jia, G., Ping, C.-L., Tape, K. D., Thompson, C. D. C., Walker, D. A., and Welker, J. M.: Role of land-surface changes in Arctic summer warming, *Science*, 310, 657–660, <https://doi.org/10.1126/science.1117368>, 2005.
- 395 Environment and Climate Change Canada: Historical data Trail Valley, Northwest Territories, [http://climate.weather.gc.ca/historical\\_data/search\\_historic\\_data\\_e.html](http://climate.weather.gc.ca/historical_data/search_historic_data_e.html), accessed 2019/01/10.
- Frost, G. V. and Epstein, H. E.: Tall shrub and tree expansion in Siberian tundra ecotones since the 1960s, *Global Change Biology*, 20, 1264–1277, <https://doi.org/10.1111/gcb.12406>, 2014.
- Frost, G. V., Epstein, H. E., Walker, D. A., Matyshak, G., and Ermokhina, K.: Patterned-ground facilitates shrub expansion in Low Arctic
- 400 tundra, *Environmental Research Letters*, 8, 015 035, <https://doi.org/10.1088/1748-9326/8/1/015035>, 2013.
- Frost, G. V., Epstein, H. E., Walker, D. A., Matyshak, G., and Ermokhina, K.: Seasonal and Long-Term Changes to Active-Layer Temperatures after Tall Shrubland Expansion and Succession in Arctic Tundra, *Ecosystems*, 21, 507–520, <https://doi.org/10.1007/s10021-017-0165-5>, 2018.
- Gisnås, K., Westermann, S., Schuler, T. V., Litherland, T., Isaksen, K., Boike, J., and Etzelmüller, B.: A statistical approach to represent small-
- 405 scale variability of permafrost temperatures due to snow cover, *The Cryosphere*, 8, 2063–2074, <https://doi.org/10.5194/tc-8-2063-2014>, 2014.



- Grünberg, I. and Boike, J.: Vegetation map of Trail Valley Creek, Northwest Territories, Canada, <https://doi.org/10.1594/PANGAEA.904270>, 2019.
- Hopkinson, C., Fox, A., Monette, S., Churchill, J., Crasto, N., and Chasmer, L.: Mackenzie Delta LiDAR collaborative research data report.,  
410 revised 03/2011, 2009.
- Kropp, H., Loranty, M. M., Natali, S. M., Kholodov, A. L., , Rocha, A., Myers-Smith, I., Abermann, J., , Blanc-Betes, E., Blok, D., Blume-Werry, G., Boike, J., , Breen, A. L., Cahoon, S. M., Christiansen, C. T., Douglas, T. A., Epstein, H. E., Frost, G. V., Goeckede, M., Høye, T. T., Mamet, S. D., O'Donnell, J. A., Olefeldt, D., Phoenix, G. K., Salmon, V. G., Sannel, B., Smith, S. L., Sonnentag, O., Vaughn, L. S., Williams, M., Elberling, B., Gough, L., Hjort, J., Lafleur, P. M., Euskirchen, E. S., Heijmans, M. M. P. D., Humphreys, E. R.,  
415 Iwata, H., Jones, B. M., Jorgenson, M. T., Grünberg, I., Kim, Y., Laundre, J., Mauritz, M., Michelsen, A., Schaepman-Strub, G., Tape, K. D., Ueyama, M., Lee, B.-Y., and Langley, K.: Vegetation stature controls air–soil temperature coupling across pan-Arctic ecosystems, submitted, 2020.
- Langer, M., Westermann, S., Heikenfeld, M., Dorn, W., and Boike, J.: Satellite-based modeling of permafrost temperatures in a tundra lowland landscape, *Remote Sensing of Environment*, 135, 12–24, <https://doi.org/10.1016/j.rse.2013.03.011>, 2013.
- 420 Lantz, T. C., Kokelj, S. V., Gergel, S. E., and Henry, G. H. R.: Relative impacts of disturbance and temperature: persistent changes in microenvironment and vegetation in retrogressive thaw slumps, *Global Change Biology*, 15, 1664–1675, <https://doi.org/10.1111/j.1365-2486.2009.01917.x>, 2009.
- Lantz, T. C., Gergel, S. E., and Henry, G. H. R.: Response of green alder (*Alnus viridis* subsp. *fruticosa*) patch dynamics and plant community composition to fire and regional temperature in north-western Canada, *Journal of Biogeography*, 37, 1597–1610,  
425 <https://doi.org/10.1111/j.1365-2699.2010.02317.x>, 2010.
- Lantz, T. C., Marsh, P., and Kokelj, S. V.: Recent shrub proliferation in the Mackenzie Delta uplands and microclimatic implications, *Ecosystems*, 16, 47–59, <https://doi.org/10.1007/s10021-012-9595-2>, 2013.
- Loranty, M. M. and Goetz, S. J.: Shrub expansion and climate feedbacks in Arctic tundra, *Environmental Research Letters*, 7, 011 005, <https://doi.org/10.1088/1748-9326/7/1/011005>, 2012.
- 430 Loranty, M. M., Abbott, B. W., Blok, D., Douglas, T. A., Epstein, H. E., Forbes, B. C., Jones, B. M., Kholodov, A. L., Kropp, H., Malhotra, A., Mamet, S. D., Myers-Smith, I. H., Natali, S. M., O'Donnell, J. A., Phoenix, G. K., Rocha, A. V., Sonnentag, O., Tape, K. D., and Walker, D. A.: Reviews and syntheses: Changing ecosystem influences on soil thermal regimes in northern high-latitude permafrost regions, *Biogeosciences*, 15, 5287–5313, <https://doi.org/10.5194/bg-15-5287-2018>, 2018.
- MacKay, J. R.: Active Layer Changes (1968 to 1993) following the Forest-Tundra Fire near Inuvik, N.W.T., Canada, *Arctic and Alpine Research*, 27, 323–336, <https://doi.org/10.1080/00040851.1995.12003129>, 1995.
- 435 Mann, P. C.: Spatial and temporal variability of the snow environment in the Western Canadian Arctic, Master's thesis, <https://scholars.wlu.ca/etd/2011/>, 2018.
- Marsh, P., Pomeroy, J., Pohl, S., Quinton, W., Onclin, C., Russell, M., Neumann, N., Pietroniro, A., Davison, B., and McCartney, S.: Snowmelt Processes and Runoff at the Arctic Treeline: Ten Years of MAGS Research, pp. 97–123, Springer Berlin Heidelberg, Berlin, Heidelberg,  
440 [https://doi.org/10.1007/978-3-540-75136-6\\_6](https://doi.org/10.1007/978-3-540-75136-6_6), 2008.
- Marsh, P., Bartlett, P., MacKay, M., Pohl, S., and Lantz, T.: Snowmelt energetics at a shrub tundra site in the western Canadian Arctic, *Hydrological Processes*, 24, 3603–3620, <https://doi.org/10.1002/hyp.7786>, 2010.



- McManus, K. M., Morton, D. C., Masek, J. G., Wang, D., Sexton, J. O., Nagol, J. R., Ropars, P., and Boudreau, S.: Satellite-based evidence for shrub and graminoid tundra expansion in northern Quebec from 1986 to 2010, *Global Change Biology*, 18, 2313–2323, 445 <https://doi.org/10.1111/j.1365-2486.2012.02708.x>, 2012.
- Michaelson, G. J., Ping, C. L., and Kimble, J. M.: Carbon Storage and Distribution in Tundra Soils of Arctic Alaska, U.S.A., *Arctic and Alpine Research*, 28, 414–424, <https://doi.org/10.1080/00040851.1996.12003194>, 1996.
- Myers-Smith, I. H., Forbes, B. C., Wilking, M., Hallinger, M., Lantz, T., Blok, D., Tape, K. D., Macias-Fauria, M., Sass-Klaassen, U., Lévesque, E., Boudreau, S., Ropars, P., Hermanutz, L., Trant, A., Collier, L. S., Weijers, S., Rozema, J., Rayback, S. A., Schmidt, N. M., 450 Schaepman-Strub, G., Wipf, S., Rixen, C., Ménard, C. B., Venn, S., Goetz, S., Andreu-Hayles, L., Elmendorf, S., Ravolainen, V., Welker, J., Grogan, P., Epstein, H. E., and Hik, D. S.: Shrub expansion in tundra ecosystems: dynamics, impacts and research priorities, *Environmental Research Letters*, 6, 045 509, <https://doi.org/10.1088/1748-9326/6/4/045509>, 2011.
- Nelson, F. E., Shiklomanov, N. I., Mueller, G. R., Hinkel, K. M., Walker, D. A., and Bockheim, J. G.: Estimating Active-Layer Thickness over a Large Region: Kuparuk River Basin, Alaska, U.S.A., *Arctic and Alpine Research*, 29, 367–378, <https://doi.org/10.2307/1551985>, 455 1997.
- Pajunen, A. M., Oksanen, J., and Virtanen, R.: Impact of shrub canopies on understorey vegetation in western Eurasian tundra, *Journal of Vegetation Science*, 22, 837–846, <https://doi.org/10.1111/j.1654-1103.2011.01285.x>, 2011.
- Palmer, M. J., Burn, C. R., and Kokelj, S. V.: Factors influencing permafrost temperatures across tree line in the uplands east of the Mackenzie Delta, 2004–2010, *Canadian Journal of Earth Sciences*, 49, 877–894, <https://doi.org/10.1139/e2012-002>, 2012.
- 460 Park, H., Kim, Y., and Kimball, J. S.: Widespread permafrost vulnerability and soil active layer increases over the high northern latitudes inferred from satellite remote sensing and process model assessments, *Remote Sensing of Environment*, 175, 349–358, <https://doi.org/10.1016/j.rse.2015.12.046>, 2016.
- Pix4D SA: Pix4Dmapper, 2019.
- Pomeroy, J. W., Marsh, P., and Gray, D. M.: Application of a distributed blowing snow model to the Arctic, *Hydrological Processes*, 11, 465 1451–1464, [https://doi.org/10.1002/\(SICI\)1099-1085\(199709\)11:11<1451::AID-HYP449>3.0.CO;2-Q](https://doi.org/10.1002/(SICI)1099-1085(199709)11:11<1451::AID-HYP449>3.0.CO;2-Q), 1997.
- Pomeroy, J. W., Bewley, D. S., Essery, R. L. H., Hedstrom, N. R., Link, T., Granger, R. J., Sicart, J. E., Ellis, C. R., and Janowicz, J. R.: Shrub tundra snowmelt, *Hydrological Processes*, 20, 923–941, <https://doi.org/10.1002/hyp.6124>, 2006.
- Quinton, W., Gray, D., and Marsh, P.: Subsurface drainage from hummock-covered hillslopes in the Arctic tundra, *Journal of Hydrology*, 237, 113–125, [https://doi.org/10.1016/S0022-1694\(00\)00304-8](https://doi.org/10.1016/S0022-1694(00)00304-8), 2000.
- 470 Stocker, T. F., Qin, D., Plattner, G.-K., Tignor, M., Allen, S. K., Boschung, J., Nauels, A., Xia, Y., Bex, V., and Midgley, P. M., eds.: *Climate Change 2013: The Physical Science Basis*, Cambridge University Press, [http://www.ipcc.ch/pdf/assessment-report/ar5/wg1/WG1AR5\\_ALL\\_FINAL.pdf](http://www.ipcc.ch/pdf/assessment-report/ar5/wg1/WG1AR5_ALL_FINAL.pdf), IPCC, 2013, 2013.
- Street, L. E., Subke, J.-A., Baxter, R., Dinsmore, K. J., Knoblauch, C., and Wookey, P. A.: Ecosystem carbon dynamics differ between tundra shrub types in the western Canadian Arctic, *Environmental Research Letters*, 13, 084 014, <https://doi.org/10.1088/1748-9326/aad363>, 475 2018.
- Sturm, M. and Holmgren, J.: An Automatic Snow Depth Probe for Field Validation Campaigns, *Water Resources Research*, 54, 9695–9701, <https://doi.org/10.1029/2018WR023559>, 2018.
- Sturm, M., Racine, C., and Tape, K.: Increasing shrub abundance in the Arctic, *Nature*, 411, 546–547, <https://doi.org/10.1038/35079180>, 2001.



- 480 Sturm, M., Schimel, J., Michaelson, G., Welker, J., Oberbauer, S., Liston, G., Fahnestock, J., and Romanovsky, V.: Winter Biological Processes Could Help Convert Arctic Tundra to Shrubland, *BioScience*, 55, 17–26, [https://doi.org/10.1641/0006-3568\(2005\)055\[0017:WBPCHC\]2.0.CO;2](https://doi.org/10.1641/0006-3568(2005)055[0017:WBPCHC]2.0.CO;2), 2005.
- Sweet, S. K., Gough, L., Griffin, K. L., and Boelman, N. T.: Tall Deciduous Shrubs Offset Delayed Start of Growing Season Through Rapid Leaf Development in the Alaskan Arctic Tundra, *Arctic, Antarctic, and Alpine Research*, 46, 682–697, <https://doi.org/10.1657/1938-4246-46.3.682>, 2014.
- 485 Tape, K., Sturm, M., and Racine, C.: The evidence for shrub expansion in Northern Alaska and the Pan-Arctic, *Global Change Biology*, 12, 686–702, <https://doi.org/10.1111/j.1365-2486.2006.01128.x>, 2006.
- Walker, D. A., Jia, G. J., Epstein, H. E., Reynolds, M. K., Chapin, III, F. S., Copass, C., Hinzman, L. D., Knudson, J. A., Maier, H. A., Michaelson, G. J., Nelson, F., Ping, C. L., Romanovsky, V. E., and Shiklomanov, N.: Vegetation – soil-thaw-depth relationships along a low-arctic bioclimate gradient, Alaska: synthesis of information from the ATLAS studies, *Permafrost and Periglacial Processes*, 14, 103–123, <https://doi.org/10.1002/ppp.452>, 2003.
- 490 Walker, D. A., Reynolds, M. K., Daniëls, F. J. A., Einarsson, E., Elvebakk, A., Gould, W. A., Katenin, A. E., Kholod, S. S., Markon, C. J., Melnikov, E. S., Moskalenko, N. G., Talbot, S. S., Yurtsev, B. A., and The other members of the CAVM Team: The Circumpolar Arctic vegetation map, *Journal of Vegetation Science*, 16, 267–282, <https://doi.org/10.1111/j.1654-1103.2005.tb02365.x>, 2005.
- 495 Walker, D. A., Epstein, H. E., Romanovsky, V. E., Ping, C. L., Michaelson, G. J., Daanen, R. P., Shur, Y., Peterson, R. A., Krantz, W. B., Reynolds, M. K., Gould, W. A., Gonzalez, G., Nicosky, D. J., Vonlanthen, C. M., Kade, A. N., Kuss, P., Kelley, A. M., Munger, C. A., Tarnocai, C. T., Matveyeva, N. V., and Daniëls, F. J. A.: Arctic patterned-ground ecosystems: A synthesis of field studies and models along a North American Arctic Transect, *Journal of Geophysical Research: Biogeosciences*, 113, G03S01, <https://doi.org/10.1029/2007JG000504>, 2008.
- 500 Wang, W., Rinke, A., Moore, J. C., Ji, D., Cui, X., Peng, S., Lawrence, D. M., McGuire, A. D., Burke, E. J., Chen, X., Decharme, B., Koven, C., MacDougall, A., Saito, K., Zhang, W., Alkama, R., Bohn, T. J., Ciais, P., Delire, C., Gouttevin, I., Hajima, T., Krinner, G., Lettenmaier, D. P., Miller, P. A., Smith, B., Sueyoshi, T., and Sherstiukov, A. B.: Evaluation of air–soil temperature relationships simulated by land surface models during winter across the permafrost region, *The Cryosphere*, 10, 1721–1737, <https://doi.org/10.5194/tc-10-1721-2016>, 2016.
- 505 Widhalm, B., Bartsch, A., Leibman, M., and Khomutov, A.: Active-layer thickness estimation from X-band SAR backscatter intensity, *The Cryosphere*, 11, 483–496, <https://doi.org/10.5194/tc-11-483-2017>, 2017.
- Wilcox, E. J., Keim, D., de Jong, T., Walker, B., Sonnentag, O., Sniderhan, A. E., Mann, P., and Marsh, P.: Tundra shrub expansion may amplify permafrost thaw by advancing snowmelt timing, *Arctic Science*, <https://doi.org/10.1139/AS-2018-0028>, accepted, 2019.
- Zhang, T.: Influence of the seasonal snow cover on the ground thermal regime: An overview, *Reviews of Geophysics*, 43, RG4002, <https://doi.org/10.1029/2004RG000157>, 2005.
- 510 Zhang, T., Osterkamp, T. E., and Stamnes, K.: Influence of the Depth Hoar Layer of the Seasonal Snow Cover on the Ground Thermal Regime, *Water Resources Research*, 32, 2075–2086, <https://doi.org/10.1029/96WR00996>, 1996.
- Zhang, Y., Olthof, I., Fraser, R., and Wolfe, S. A.: A new approach to mapping permafrost and change incorporating uncertainties in ground conditions and climate projections, *The Cryosphere*, 8, 2177–2194, <https://doi.org/10.5194/tc-8-2177-2014>, 2014.
- 515 Zhang, Y., Sherstiukov, A. B., Qian, B., Kokelj, S. V., and Lantz, T. C.: Impacts of snow on soil temperature observed across the circumpolar north, *Environmental Research Letters*, 13, 044 012, <https://doi.org/10.1088/1748-9326/aab1e7>, 2018.

<https://doi.org/10.5194/bg-2020-88>  
Preprint. Discussion started: 30 March 2020  
© Author(s) 2020. CC BY 4.0 License.



Zwieback, S., Chang, Q., Marsh, P., and Berg, A.: Shrub tundra ecohydrology: rainfall interception is a major component of the water balance, *Environmental Research Letters*, <https://doi.org/10.1088/1748-9326/ab1049>, 2019.